AMERICAN SOCIETY FOR MICROBIOLOGY | Microbiology Spectrum

RESEARCH ARTICLE

Proton Motive Force Inhibitors Are Detrimental to Methicillin-Resistant *Staphylococcus aureus* Strains

Sayed Golam Mohiuddin,[a] Sreyashi Ghosh,[a] Pouria Kavousi,[a] Mehmet A. Orman[a]

[a]Department of Chemical and Biomolecular Engineering, University of Houston, Houston, Texas, USA

ABSTRACT Methicillin-resistant *Staphylococcus aureus* (MRSA) strains are tolerant of conventional antibiotics, making them extremely dangerous. Previous studies have shown the effectiveness of proton motive force (PMF) inhibitors at killing bacterial cells; however, whether these agents can launch a new treatment strategy to eliminate antibiotic-tolerant cells mandates further investigation. Here, using known PMF inhibitors and two different MRSA isolates, we showed that the bactericidal potency of PMF inhibitors seemed to correlate with their ability to disrupt PMF and permeabilize cell membranes. By screening a small chemical library to verify this correlation, we identified a subset of chemicals (including nordihydroguaiaretic acid, gossypol, trifluoperazine, and amitriptyline) that strongly disrupted PMF in MRSA cells by dissipating either the transmembrane electric potential ($\Delta\Psi$) or the proton gradient (ΔpH). These drugs robustly permeabilized cell membranes and reduced MRSA cell levels below the limit of detection. Overall, our study further highlights the importance of cellular PMF as a target for designing new bactericidal therapeutics for pathogens.

IMPORTANCE Methicillin-resistant *Staphylococcus aureus* (MRSA) emerged as a major hypervirulent pathogen that causes severe health care-acquired infections. These pathogens can be multidrug-tolerant cells, which can facilitate the recurrence of chronic infections and the emergence of diverse antibiotic-resistant mutants. In this study, we aimed to investigate whether proton motive force (PMF) inhibitors can launch a new treatment strategy to eliminate MRSA cells. Our in-depth analysis showed that PMF inhibitors that strongly dissipate either the transmembrane electric potential or the proton gradient can robustly permeabilize cell membranes and reduce MRSA cell levels below the limit of detection.

KEYWORDS methicillin-resistant *Staphylococcus aureus*, proton motive force, tolerant cells, membrane permeabilization, PMF inhibitors, high-throughput drug screening

The discovery of antibiotics in the 1940s was one of the most significant breakthroughs in therapeutic medicine. However, the medicinal potency of these life-saving drugs has been drastically reduced by the emergence of new antibiotic-resistant mutant strains. The continuous evolution of pathogens to develop resistance against antibiotics, together with the decreased rate of antibiotic discovery, might eventually cause serious public health problems, as epidemics associated with resistant pathogens may be imminent.

Staphylococcus aureus is an opportunistic Gram-positive bacterial pathogen that colonizes human skin and mucous membranes, causing chronic, recurrent infections, including wound infections, bacteremia, and biofilm infections (1, 2). Methicillin, a narrow-spectrum β-lactam antibiotic, was introduced in the late 1950s to treat infections caused by penicillin-resistant *S. aureus* (3). Unfortunately, accession of the methicillin-resistance gene, *mecA*, encoding an alternative penicillin-binding protein, makes *S. aureus* infections extremely difficult to treat (4). Methicillin-resistant *S. aureus* (MRSA) emerged as a major hypervirulent pathogen that causes severe health care-acquired infections, such as surgical site infections, hospital-acquired pneumonia, catheter-associated urinary tract infections, central line-associated bloodstream infections, and ventilator-associated pneumonia (5). Almost 19,000 people

Editor Silvia T. Cardona, University of Manitoba

Address correspondence to Mehmet A. Orman, morman@central.uh.edu.

The authors declare no conflict of interest.

Received 8 June 2022
Accepted 8 July 2022
Published 9 August 2022

die annually as a consequence of MRSA infections in the United States alone (6). Approximately 20% of patients in the United States contract at least one nosocomial infection while undergoing surgery, which adds $5 to 10 billion in costs to the U.S. health care system (7, 8).

The cell membrane is an essential cellular component and might be a good target for novel bactericidal therapeutics (9). The bacterial proton motive force (PMF) maintains the electrochemical proton gradient across the cell membrane, an essential component of ATP synthesis (9, 10). The electric potential ($\Delta\Psi$) and the transmembrane proton gradient (ΔpH) are the two components of PMF. Cells can compensate for the dissipation of one component by enhancing the other to maintain the necessary level of PMF (11). A number of chemicals disrupt the PMF of *S. aureus* by dissipating either $\Delta\Psi$ or ΔpH (12–14). Halicin is a potential broad-spectrum antibacterial molecule that selectively dissipates ΔpH (13). The small molecule JD1 disrupts $\Delta\Psi$, kills MRSA cells, and significantly reduces biofilm formation (14). Bedaquiline, SQ109, pyrazinamide, clofazimine, nitazoxanide, and 2-aminoimidazoles are also potent PMF inhibitors in Gram-positive bacteria (12, 15). PMF inhibitors can also permeabilize the membranes of bacterial cells through interactions with phospholipids or membrane-bound proteins (16–18). Polymyxin B, a well known inhibitor of $\Delta\Psi$, perturbs the cell membranes of bacteria by binding lipopolysaccharides (9, 19).

Although the effectiveness of PMF inhibitors against bacterial cells has been highlighted in prior studies (9, 13, 16, 19–23), whether PMF inhibitors can be used as a potent bactericidal for MRSA strains necessitates further investigation. Therefore, in this study, we sought to determine whether disrupting PMF of MRSA can be detrimental for these cells. Because electron transport chain (ETC) complexes are highly conserved across species, we used a small library of 22 chemical compounds that inhibit various mitochondrial ETC complexes and identified several drugs (nordihydroguaiaretic acid, gossypol, trifluoperazine, and amitriptyline) that disrupted PMF in MRSA strains by dissipating either ΔpH or $\Delta\Psi$. Although most of these chemicals drastically reduced MRSA survival compared with conventional antibiotics, our subsequent analysis verified that the extent of PMF disruption and membrane permeabilization is a key factor determining the treatment outcome.

RESULTS

PMF inhibitors can effectively kill MRSA strains. First, we tested the effectiveness of known PMF inhibitors, such as polymyxin B, thioridazine, and carbonyl cyanide *m*-chlorophenyl hydrazone (CCCP), on MRSA tolerance in two isolates: MRSA BAA-41 and MRSA 700699. Polymyxin B is a cationic peptide that electrostatically binds the negatively charged moieties of lipopolysaccharides, disrupting $\Delta\Psi$ and permeabilizing the cell membrane (24). Thioridazine, an antipsychotic drug, disrupts $\Delta\Psi$ in Gram-positive bacteria, potentially by blocking NADH:quinone oxidoreductase II (NDH-II) (18, 25). CCCP is a protonophore that transports hydrogen ions across the cell membrane, subsequently reducing ATP production and disrupting PMF (26).

Dissipation of either $\Delta\Psi$ or ΔpH by inhibitors may cause the eventual collapse of the bacterial cellular PMF and disrupt membrane integrity (9). To assess the effects of PMF inhibitors on membrane permeability, strains MRSA BAA-41 and MRSA 700699 were grown to an optical density at 600 nm (OD_{600}) of ~0.1 in Mueller-Hinton broth in test tubes (Fig. S1); treated with polymyxin B, thioridazine, or CCCP at 5× or 10× of the MIC for 1 h (Table S1A); and then stained with propidium iodide (PI). PI is a membrane-impermeant DNA- and RNA-binding dye that can stain only the nucleic acids of cells with compromised membranes. Flow cytometric analysis of PI-stained cells revealed that polymyxin B at 5× and 10× MIC permeabilized more than 80% of MRSA BAA-41 cells (Fig. 1A; Table S2A) but less than 80% of MRSA 700699 cells (Fig. 2A; Table S2A). Although robust membrane permeabilization was not observed after CCCP treatment at the indicated concentrations in either strain (Fig. 1A and 2A; Table S2A), thioridazine treatment at 5× and 10× MIC permeabilized more than 90% of cells of both strains (Fig. 1A and 2A; Table S2A).

To determine whether the observed membrane permeabilization was linked to the perturbation of PMF, we used the potentiometric probe 3,3′-dipropylthiadicarbocyanine iodide

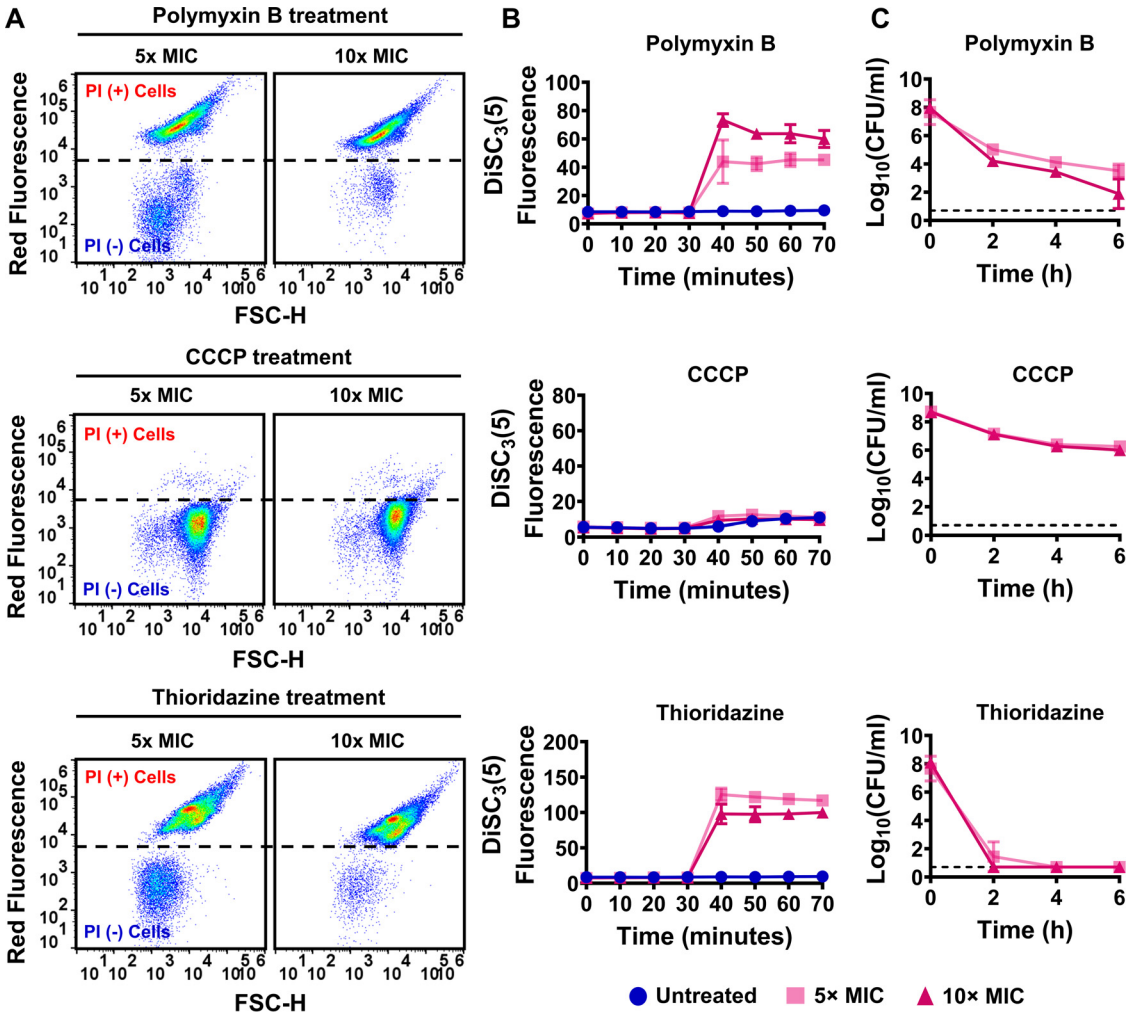

FIG 1 Proton motive force (PMF) inhibitors increased membrane permeability, disrupted cellular PMF, and reduced cell survival levels in strain MRSA BAA-41. (A) MRSA BAA-41 cells were grown to the exponential phase (optical density at 600 nm [OD_{600}] of ~0.1) in Mueller-Hinton broth and treated with polymyxin B, carbonyl cyanide *m*-chlorophenyl hydrazone (CCCP), or thioridazine at concentrations of 5× and 10× MIC (Table S1A). After 1 h treatment, the cells were collected and stained with propidium iodide (PI) (20 μM) dye for flow cytometry analysis. Live and ethanol-treated (70%, vol/vol) dead cells were used as negative (–) and positive (+) controls (Fig. S2). A representative flow cytometry diagram is shown here; all independent biological replicates produced similar results. (B) Cells grown to the exponential phase (OD_{600} of ~0.1) were transferred to 3,3′-dipropylthiadicarbocyanine iodide ($DiSC_3[5]$) assay buffer (50 mM HEPES, 300 mM KCl, and 0.1% glucose) and stained with $DiSC_3(5)$. When the cells reached an equilibrium state (t = 30 min), they were treated with polymyxin B, CCCP, or thioridazine at the indicated concentrations. The fluorescence levels were measured with a plate reader at the designated time points. Cultures stained with the $DiSC_3(5)$ but not treated with PMF inhibitors were used as control. (C) Cells at the exponential phase (OD_{600} of ~0.1) were treated with the drugs at the indicated concentrations for 6 h. At designated time points during treatments, cells were collected, washed to remove the chemicals, and spotted on Mueller-Hinton agar plates to enumerate the colony forming units (CFU). The dashed lines in panel C indicate the limit of detection. The number of biological replicates (n) = 3. The data points represent means ± SD. FSC-H, Forward scatter.

($DiSC_3[5]$) (see Materials and Methods), which accumulates on polarized membranes and self-quenches its fluorescence (9, 13). Hyperpolarization due to perturbation of ΔpH enhances the accumulation of $DiSC_3(5)$ and reduces the fluorescence signals, whereas disruption of $\Delta\Psi$ increases fluorescence by releasing the probe into the medium (9, 13). Polymyxin B at 5× and 10× MIC disrupted the cellular PMF by selectively dissipating $\Delta\Psi$ in both strains in a concentration-dependent manner (Fig. 1B and 2B; Table S2A). The dissipation of $\Delta\Psi$ was greater in thioridazine-treated cultures than in polymyxin B-treated cultures (Fig. 1B and 2B; Table S2A). Thioridazine at 10× MIC increased the $DiSC_3(5)$ fluorescence level more than 11-fold in MRSA BAA-41 cells and more than 14-fold in MRSA 700699 cells compared to untreated controls (Fig. 1B and 2B; Table S2A). Despite being a proton ionophore that promptly dissipates the cellular PMF of many Gram-positive and Gram-negative bacteria (26, 27), CCCP at

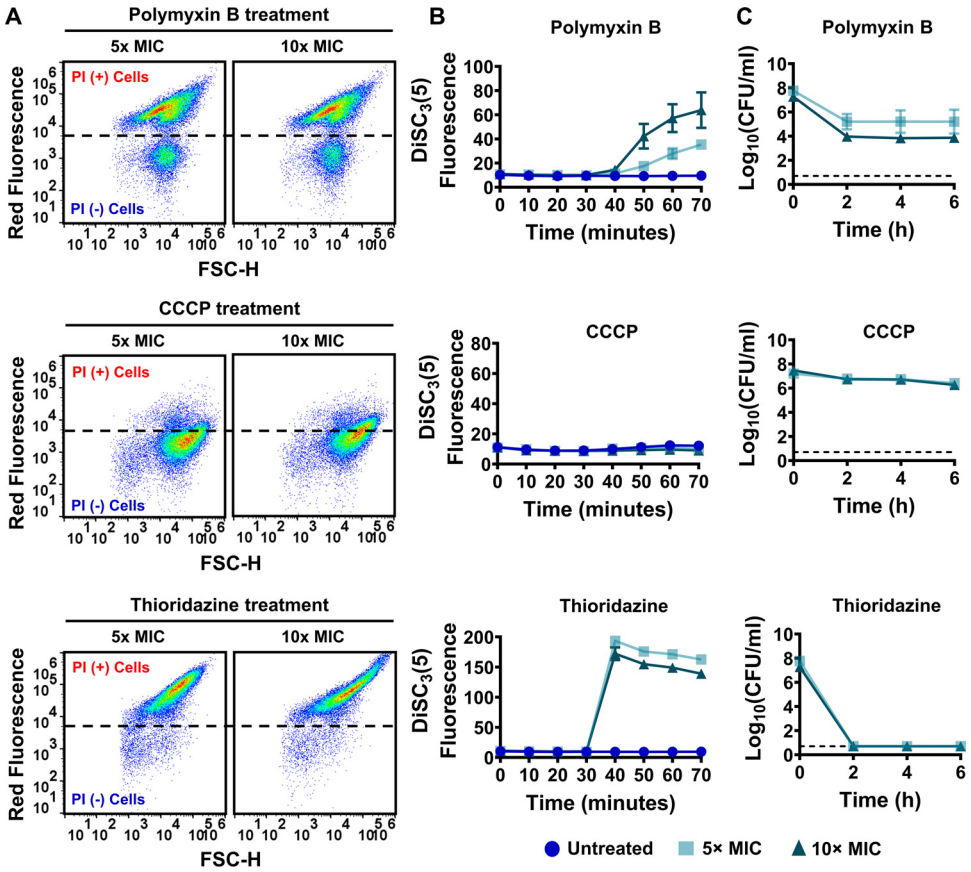

FIG 2 PMF inhibitors increased membrane permeability, disrupted cellular PMF, and reduced cell survival levels in strain MRSA 700699. Effects of polymyxin B, CCCP, and thioridazine treatments on cell membranes (A), PMF (B), and cell survival levels (C) of MRSA 700699 cells were determined as described in the legend to Fig. 1. A representative flow cytometry diagram is shown here; all independent biological replicates (n = 3) produced similar results. The dashed lines in panel C indicate the limit of detection. The data points represent means ± SD.

5× and 10× MIC did not disrupt PMF in either strain (Fig. 1B and 2B; Table S2A). Higher CCCP concentrations might be required for an effective outcome.

We performed clonogenic survival assays to assess the effectiveness of these PMF inhibitors as bactericidal drugs. MRSA BAA-41 and MRSA 700699 cells were treated with the inhibitors at 5× and 10× MIC for 6 h to generate kill curves. These assays revealed that CCCP was ineffective against MRSA strains, and polymyxin B was unable to eradicate MRSA cells after 6 h of treatment at the tested concentrations (Fig. 1C and 2C). However, thioridazine, which disrupted cell membranes and PMF to a greater extent than the other tested drugs, reduced CFU levels of both strains to below the limit of detection at both concentrations tested (Fig. 1C and 2C). Although a direct comparison of the effects of these three inhibitors on bacterial cell physiology, including their effects on MRSA tolerance, might be difficult to obtain due to the concentration-dependent nature of these effects, our data show that the conditions that lead to enhanced membrane permeabilization and PMF disruption may completely kill MRSA cells.

MRSA strains are highly tolerant of conventional antibiotics. Next, we investigated whether similar correlations between membrane integrity, PMF levels, and cell survival are observed when cells are treated with conventional antibiotics. We selected seven antibiotics, including kanamycin and gentamicin (aminoglycosides that inhibit protein biosynthesis by binding to the 30S ribosomal subunit) (28), ampicillin (a β-lactam that inhibits cell wall biosynthesis by binding to penicillin-binding proteins) (29), ofloxacin and ciprofloxacin (quinolone antibiotics that block DNA synthesis by inhibiting DNA gyrase/topoisomerase) (30), fosfomycin (a phosphonic acid that blocks cell wall biosynthesis by inhibiting the initial step involving phosphoenolpyruvate synthetase) (31), and vancomycin (a glycopeptide antibiotic that inhibits

cell wall biosynthesis by binding to the growing peptide chain) (32). Using commercial strips, we confirmed that the MICs of kanamycin, gentamicin, ampicillin, ofloxacin, ciprofloxacin, fosfomycin, and vancomycin for strain MRSA BAA-41 were within the standard test ranges (Table S1B). As kanamycin and gentamicin have similar modes of action, kanamycin was selected for clonogenic survival assays for this strain. MICs of ampicillin, ofloxacin, ciprofloxacin, and vancomycin were detectable for strain MRSA 700699, but this strain exhibited high resistance to kanamycin, gentamicin, and fosfomycin. We were unable to determine the MICs of these three antibiotics for strain MRSA 700699, which exceeded the standard test ranges (Table S1B).

Exponential-phase cells (OD_{600} of ~0.1) (Fig. S1) of strains MRSA BAA-41 and MRSA 700699 were treated with conventional antibiotics at 5× and 10× MIC (Table S1B) for PI staining, $DiSC_3(5)$, and clonogenic survival assays as described above. MRSA BAA-41 was highly tolerant of kanamycin, ofloxacin, and ciprofloxacin, and these antibiotics neither permeabilized the cytoplasmic membrane nor dissipated the PMF of this strain at the concentrations tested (Fig. S3A to C). Ampicillin, fosfomycin, and vancomycin were able to permeabilize the cell membrane without altering the PMF of strain MRSA BAA-41 but did not eradicate the MRSA cells of this strain at the concentrations tested (Fig. S3A to C). Similar trends were observed for strain MRSA 700699 (Fig. S4A to C). Although ampicillin and vancomycin significantly permeabilized MRSA 700699 cells, at the concentrations tested, none of the antibiotics altered the cellular PMF or eradicated tolerant cells of this strain (Fig. S4A to C). Altogether, the results of PMF inhibitor and conventional antibiotic treatments suggest that chemicals that increase both PMF dissipation and membrane permeabilization might be effective bactericidal drugs. However, a statistical analysis is necessary to clarify whether PMF dissipation and membrane permeabilization can truly predict cell survival.

Simple multivariable regression analysis identifies a linear correlation between independent and response variables. The patterns we observed among membrane permeabilization, PMF dissipation, and cell survival after treatment with known PMF inhibitors and conventional antibiotics suggest a correlation between these parameters. When we generated a membrane permeability versus PMF disruption plot using data from all independent biological replicates for all combinations of MRSA strains and drug concentrations (Fig. 3A), we observed two distinct clusters. The first cluster in this two-dimensional plot (Fig. 3A, red oval) primarily represents the data points corresponding to conventional antibiotics. Although some of these antibiotics (e.g., ampicillin, fosfomycin, and vancomycin) permeabilized cell membranes, they did not necessarily dissipate cellular PMF, indicating that these two parameters are not always related. The second cluster (Fig. 3A, blue oval) comprises the drugs that perturb PMF (e.g., thioridazine and polymyxin B). These drugs drastically permeabilized the cell membranes of both strains independent of PMF disruption and were more effective against MRSA cells than the drugs in the first cluster (Fig. 3A). The data on chemicals in the second cluster may indicate either a lack of correlation between membrane permeabilization and PMF disruption or the existence of a threshold level for PMF disruption that leads to drastic membrane permeabilization. If we assume that PMF dissipation and membrane permeabilization are two independent variables and the cell survival outcome is the response variable, then the potential two-way interaction between the independent variables should be statistically verifiable.

Our three-dimensional scatterplot of membrane permeability, PMF disruption, and cell survival data may indicate a linear correlation between the independent and response variables (Fig. 3B). To test whether a two-way interaction exists between the independent variables, we performed a simple multivariable correlation analysis in which the response is predicted by the independent variables using two different linear model equations with or without an interaction term (β_3; Fig. 3C and D). The first model equation without the interaction term indicates that PMF disruption has a significant effect on cell survival ($P < 0.0001$), but membrane permeability has a comparatively smaller effect ($P = 0.2067$) (Fig. 3C, D). Although the analysis associated with the second model equation may suggest the existence of interaction between the independent variables, the F statistics used to compare the model equations indicate that the first model fits the experimental data better than the second model ($P < 0.01$) (Fig. 3C, D). However, both regression

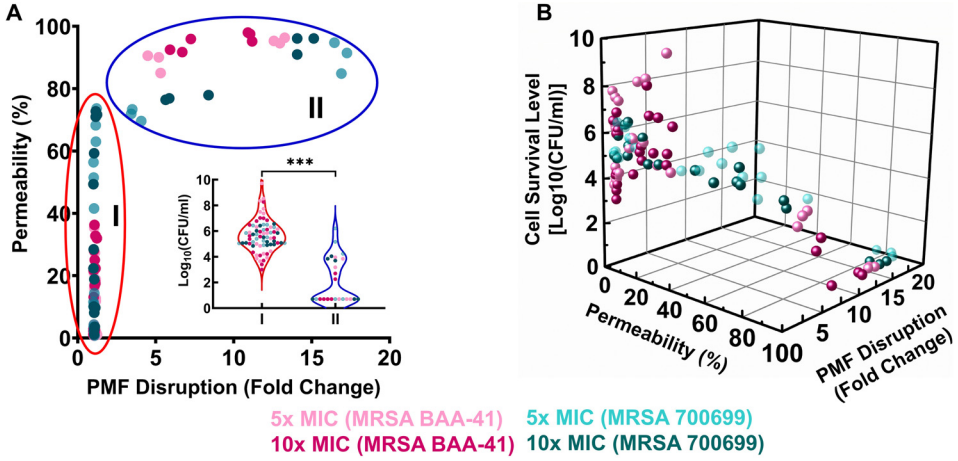

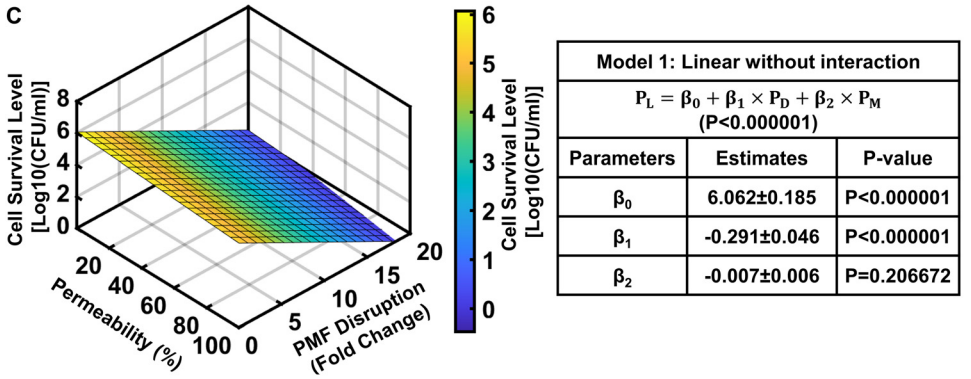

Model 1: Linear without interaction		
$P_L = \beta_0 + \beta_1 \times P_D + \beta_2 \times P_M$ (P<0.000001)		
Parameters	**Estimates**	**P-value**
β_0	6.062±0.185	P<0.000001
β_1	-0.291±0.046	P<0.000001
β_2	-0.007±0.006	P=0.206672

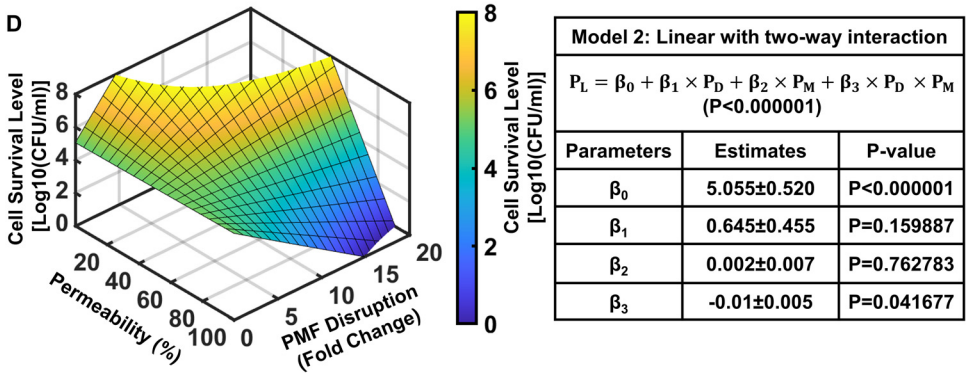

Model 2: Linear with two-way interaction		
$P_L = \beta_0 + \beta_1 \times P_D + \beta_2 \times P_M + \beta_3 \times P_D \times P_M$ (P<0.000001)		
Parameters	**Estimates**	**P-value**
β_0	5.055±0.520	P<0.000001
β_1	0.645±0.455	P=0.159887
β_2	0.002±0.007	P=0.762783
β_3	-0.01±0.005	P=0.041677

FIG 3 Simple multivariable regression analysis correlates the disruption of PMF and membrane permeability to cell survival levels. (A, B) Two- and three-dimensional scatterplots including all data points for PMF inhibitors and conventional antibiotics for all concentrations and strains tested. In panel A, the red oval indicates cluster I, and the blue oval indicates cluster II. The cell survival levels corresponding to each cluster are presented in the inset. A Student's *t* test with unequal variance was used to find the statistical significance between the cell survival levels of clusters I and II. ***, $P < 0.0001$. (C) Multivariable linear regression analysis without an interaction between the independent variables. (D) Multivariable linear regression with a two-way interaction between the independent variables. P_L = cell survival level; P_D = PMF disruption; P_M = membrane permeabilization; β_0 = the estimate of the model intercept; β_1 = the estimate of the model coefficient of PMF disruption; β_2 = the estimate of the model coefficient of membrane permeability; β_3 = the estimate of the model coefficient of the interaction term. F statistics were used for the statistical analysis with the threshold value set to $P = 0.01$.

models fit the experimental data better than a model that contains no independent variables ($P < 0.00001$).

Our experimental data, together with the statistical analysis, demonstrate the importance of cellular PMF dissipation on MRSA survival, regardless of the strains used. Although these model equations may not predict the exact number of MRSA cells surviving the treatments, they may predict the conditions necessary to reduce the level of survived cells to below the

limit of detection. When we calculated the minimum PMF disruption required to eradicate MRSA cells if 90% of the cells are assumed to be permeabilized, the first and second model equations revealed that disruption of at least 16.22 ± 4.72-fold and 17.85 ± 3.91-fold PMF, respectively, is required to reduce MRSA survival levels to below the limit of detection (5 CFU/mL), which is consistent with our experimental data (Fig. 1 and 2). However, whether PMF inhibitors can truly be used as bactericidal drugs requires further validation, as our current analysis includes a limited number of PMF inhibitors.

High-throughput screening identified new PMF inhibitors for the MRSA strains. To identify additional PMF inhibitors, we screened a small chemical library, MitoPlate I-1, containing 22 mitochondrial inhibitors. Each chemical was tested at four different concentrations in the wells of a 96-well plate. These chemicals included complex I inhibitors (rotenone and pyridaben), complex II inhibitors (malonate and carboxin), complex III inhibitors (antimycin A and myxothiazol), uncouplers (trifluoromethoxy carbonylcyanide phenylhydrazone [FCCP] and 2,4-dinitrophenol), ionophores (valinomycin and calcium chloride), and other chemicals (gossypol, nordihydroguaiaretic acid, polymyxin B, amitriptyline, meclizine, berberine, alexidine, phenformin, diclofenac, celastrol, trifluoperazine, and papaverine) that directly or indirectly inhibit the ETC of mitochondria (33–44). Although this library was specifically designed for mammalian cells, we reasoned that some of the chemicals might be effective for bacteria as the ETC is evolutionarily conserved (45). Exponential-phase cells (OD_{600} of ~0.1) of strains MRSA BAA-41 and MRSA 700699 were used to perform the $DiSC_3(5)$ assay for our initial screening. For both strains, alexidine, diclofenac, celastrol, trifluoperazine, and amitriptyline selectively dissipated $\Delta\Psi$ (increase in $DiSC_3[5]$ fluorescence levels compared to untreated control), whereas nordihydroguaiaretic acid and gossypol selectively dissipated ΔpH (decrease in $DiSC_3[5]$ fluorescence levels compared to untreated control) (Fig. S5 and S6). FCCP and antimycin A particularly disrupted the PMF in strain MRSA BAA-41 (Fig. S5).

We performed PI staining, $DiSC_3(5)$, and clonogenic survival assays to verify the reproducibility and efficacy of the identified chemicals against MRSA cells. Exponential-phase cells (OD_{600} of ~0.1) of strains MRSA BAA-41 and MRSA 700699 were treated with the identified drugs at 5× and 10× MIC. A 2-fold macrodilution method (46) was used to determine the MICs of these drugs (Table 1). The MIC of antimycin A is much higher than the range we tested (0.0078125 to 2 mM); therefore, antimycin A was not tested in the clonogenic survival assays. Our results showed that nordihydroguaiaretic acid and gossypol drastically perturbed the PMF by dissipating ΔpH, robustly permeabilized cell membranes, and reduced cell survival levels to below the limit of detection within 6 h of treatment at the concentrations tested for both MRSA BAA-41 and MRSA 700699 (Fig. 4A to C and 5A to C). The potency of gossypol in targeting cellular PMF seemed to be quite high, as it reduced $DiSC_3(5)$ fluorescence levels more than 122-fold at 10× MIC compared to untreated cells (Fig. 4B and 5B; Table S2C). Trifluoperazine and amitriptyline similarly reduced cell survival levels to below the limit of detection for both strains; however, these drugs potentially permeabilized the cell membrane by dissipating $\Delta\Psi$ (Fig. 4A to C and 5A to C). Alexidine, FCCP, diclofenac, and celastrol affected cell survival levels, cellular PMF, and membrane permeabilization in a concentration-dependent manner for both strains (Fig. S7A to C and S8A to C). Although conditions that drastically disrupted cellular PMF and permeabilized the membrane (e.g., alexidine treatment at 10× MIC) reduced cell survival levels to below the limit of detection (Fig. S7A to C and S8A to C; Table S2C), conditions that barely perturbed PMF and cell membrane permeabilization (e.g., celastrol treatments at 5× and 10× MIC) were ineffective in eliminating MRSA cells (Fig. S7A to C and S8A to C; Table S2C).

The results of our screening assay support our initial analysis, highlighted in Fig. 3. When we repeated our statistical analysis by combining the new and initial data sets of independent variables (PMF disruption and membrane permeability) for all drugs and conditions, we found that the first model (without a two-way interaction) fit the experimental data better than the second model ($P < 0.01$) (Fig. S9A, B). Although both PMF disruption and membrane permeability had significant effects on cell survival ($P < 0.0001$), the effects of interactions between PMF and membrane permeability on cell survival were insignificant with the addition of new data ($P = 0.1495$). Altogether, our results verified that

TABLE 1 MICs of identified PMF inhibitors[a]

Identified PMF Inhibitors[b]			
PMF inhibitors	**Bacterial strains**	**MIC (mM)**	**Clonogenic survival assay concentrations (mM)**
Nordihydroguaiaretic acid	MRSA BAA-41	0.0375 ± 0.025	0.1875 (5 × MIC) 0.375 (10 × MIC)
	MRSA 700699	0.0375 ± 0.025	0.1875 (5 × MIC) 0.375 (10 × MIC)
Gossypol	MRSA BAA-41	0.023 ± 0.008	0.115 (5 × MIC) 0.23 (10 × MIC)
	MRSA 700699	0.023 ± 0.008	0.115 (5 × MIC) 0.23 (10 × MIC)
Trifluoperazine	MRSA BAA-41	0.05 ± 0.015	0.25 (5 × MIC) 0.5 (10 × MIC)
	MRSA 700699	0.05 ± 0.015	0.25 (5 × MIC) 0.5 (10 × MIC)
Amitriptyline	MRSA BAA-41	0.75 ± 0.25	3.75 (5 × MIC) 7.5 (10 × MIC)
	MRSA 700699	0.375 ± 0.125	1.875 (5 × MIC) 3.75 (10 × MIC)
Alexidine	MRSA BAA-41	0.000183 ± 0.00006	0.000915 (5 × MIC) 0.00183 (10 × MIC)
	MRSA 700699	0.000366 ± 0.000122	0.00183 (5 × MIC) 0.00366 (10 × MIC)
FCCP	MRSA BAA-41	0.003 ± 0.001	0.015 (5 × MIC) 0.03 (10 × MIC)
Diclofenac	MRSA BAA-41	0.75 ± 0.25	3.75 (5 × MIC) 7.5 (10 × MIC)
	MRSA 700699	0.75 ± 0.25	3.75 (5 × MIC) 7.5 (10 × MIC)
Celastrol	MRSA BAA-41	0.00073 ± 0.00024	0.00365 (5 × MIC) 0.0073 (10 × MIC)
	MRSA 700699	0.006 ± 0.002	0.03 (5 × MIC) 0.06 (10 × MIC)
Antimycin A	MRSA BAA-41	>2	N/A

[a]PMF, proton motive force; MRSA, methicillin-resistant *S. aureus*; FCCP, trifluoromethoxy carbonylcyanide phenylhydrazone; N/A, not applicable.
[b]A 2-fold macrodilution method was used to determine the MICs.

conditions leading to robust disruption of PMF and drastic cell membrane permeabilization could reduce cell survival levels to below the limit of detection.

DISCUSSION

In this study, the strains MRSA BAA-41 and MRSA 700699 were employed to explore the disruption of PMF as a potential therapeutic approach against MRSA cells. These strains are *S. aureus* clinical isolates that are intrinsically resistant to methicillin (47, 48). MRSA BAA-41 was isolated from a patient in a New York City hospital in 1994 (47). MRSA 700699 was isolated from the pus and debrided tissue that developed at a surgical incision in the sternum of an infant from Japan (48). The two strains have different growth rates—MRSA BAA-41 proliferates faster than MRSA 700699 in Mueller-Hinton broth (Fig. S1)—and are both highly tolerant of conventional antibiotics.

Resistance is a phenomenon that describes the ability of bacteria to survive and proliferate in the presence of antibiotics (49–51). Resistance is an inheritable attribute that cells can acquire through numerous mechanisms, including horizontal gene transfers and/or mutations altering antibiotic target sites (52, 53). This trait enables cells to decrease the potency of antibiotics; therefore, higher doses are necessary to produce the bactericidal effect against cells (49, 50). The resistance level is commonly measured by the MIC, the lowest antibiotic concentration needed to prevent bacterial growth (49, 50). In this study, we treated the cells with antibiotic concentrations higher than MIC (5× and 10× MIC); hence, we did not use the "resistant" term to define the cell subpopulations surviving the drug treatments. Tolerance, on the other hand, is defined as the ability of any bacterial strain to withstand a

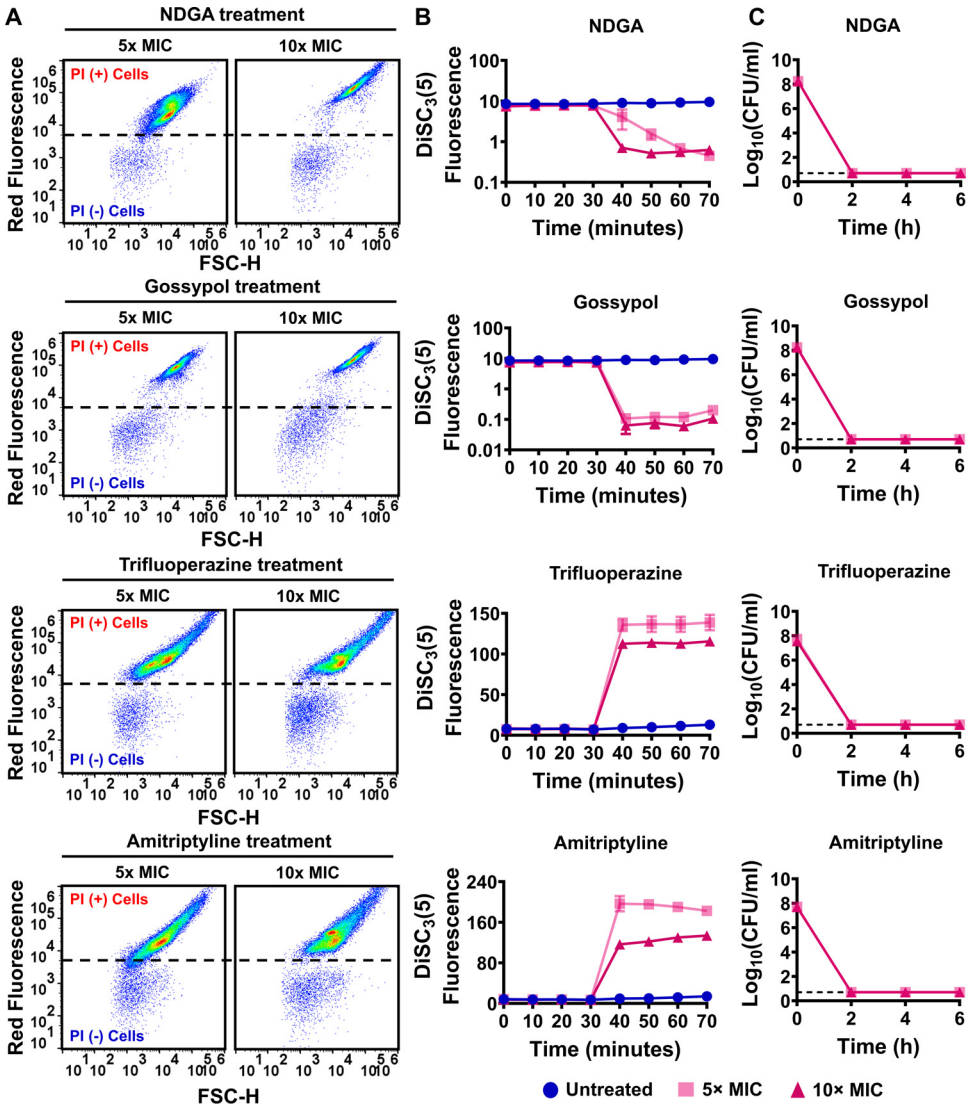

FIG 4 The identified drugs increased membrane permeability, disrupted cellular PMF, and reduced cell survival levels in strain MRSA BAA-41. The effects of nordihydroguaiaretic acid (NDGA), gossypol, trifluoperazine, and amitriptyline treatments on cell membranes (A), PMF (B), and cell survival levels (C) of MRSA BAA-41 cells were determined as described in the legend to Fig. 1. A representative flow cytometry diagram is shown here; all independent biological replicates (n = 3) produced similar results. The dashed lines in panel C indicate the limit of detection. The data points represent means ± SD.

transient exposure to bactericidal antibiotics (50, 51). Most importantly, tolerant cells survive the treatment without having an increase in MIC levels (50). The minimum duration of killing (MDK_{99}) is used to quantify the tolerance level, defined as the time required to kill 99% of cells of the culture at a concentration higher than the MIC (49, 50). Researchers put forward another way of measuring the tolerance level by using the ratio of MBC to MIC, in which the MBC is the minimum bactericidal concentration that can kill 99.9% of bacteria after 24 h of exposure (50). Antibiotic persistence is another phenomenon in which a small isogenic subpopulation of cultures can temporarily tolerate lethal concentrations of an antibiotic without increasing the MIC significantly (49, 50, 54). The presence of persisters can be detected by a biphasic kill curve, in which the initial rapid killing regime represents the death of normal cells, and the plateau with a lower killing rate indicates the presence of persisters within the culture (49, 54). Tolerance and persistence are nonheritable strategies adopted by microorganisms, and in some cases, these terms are used interchangeably (49, 50, 54). This article focused on the general ability of a cell culture to tolerate antibiotic concentrations higher than the MIC levels; hence, we used the terms "tolerance" and "tolerant cells" throughout the article.

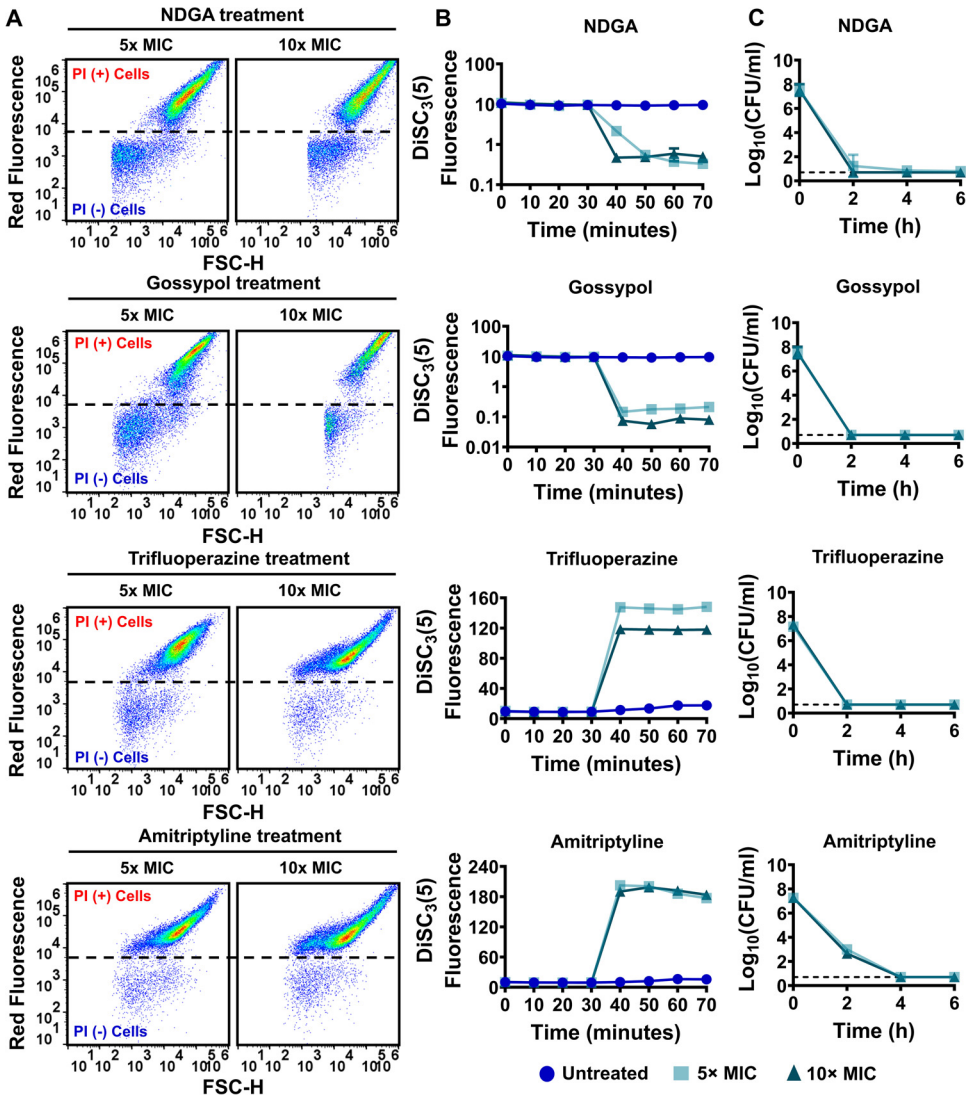

FIG 5 The identified drugs increased membrane permeability, disrupted cellular PMF, and reduced cell survival levels in strain MRSA 700699. The effects of nordihydroguaiaretic acid (NDGA), gossypol, trifluoperazine, and amitriptyline treatments on cell membranes (A), PMF (B), and cell survival levels (C) of MRSA 700699 cells were determined as described in the legend to Fig. 1. A representative flow cytometry diagram is shown here; all independent biological replicates (n = 3) produced similar results. The dashed lines in panel C indicate the limit of detection. The data points represent means ± SD.

PMF is crucial for bacterial cell growth and survival under normal and/or stress conditions (26). As the driving force for ATP synthesis via F1F0-ATPase (26), PMF provides the necessary energy for many intracellular processes, forming the Achilles heel of living organisms; therefore, the dissipation of one of its components ($\Delta\Psi$ or ΔpH) can dismantle the cellular adenylate energy charge and kill bacteria (9). Our initial data sets obtained from known PMF inhibitors and conventional antibiotics highlight a strong correlation between cellular membrane permeabilization, PMF disruption, and cell survival levels in MRSA strains. Our statistical analysis demonstrated that two independent variables (membrane permeabilization and PMF disruption) had a significant effect on the response variable (cell survival levels). We further showed that the response variable can be defined by a linear regression model with an insignificant two-way interaction between the independent variables. However, this lack of statistical interaction does not necessarily imply that PMF and membrane integrity are not related. PMF inhibitors seem to permeabilize cell membranes either completely (e.g., thioridazine) or not at all (e.g., CCCP), depending on their potency; therefore, permeabilization mediated by PMF inhibitors could potentially occur above a certain

potency threshold. Because our experimental results and data analysis suggest that PMF inhibitors can be effective bactericidal drugs for MRSA strains, we screened a small chemical library containing 22 mitochondrial inhibitors and found that several drugs, including nordihydroguaiaretic acid, gossypol, trifluoperazine, amitriptyline, and alexidine, were effective PMF inhibitors for MRSA strains and could robustly permeabilize the cell membrane and reduce cell survival levels to below the limit of detection.

The chemicals in the library inhibit different mechanisms of the mitochondrial ETC system (33–44, 55–57). The ETC is evolutionarily conserved across species (45), which may explain the observed high hit rate achieved by screening a small chemical library. As cancer cells are characterized by increased proliferation and mitochondrial activities, these drugs are effective inhibitors for many cancer cells. Gossypol is a naturally occurring aldehyde extracted from a cotton plant that inhibits two fragments of mitochondrial electron transfer and triggers the production of reactive oxygen species (36), which have antitumor effects against several myeloma cells by inducing apoptosis (58). Trifluoperazine is an antipsychotic drug that dissipates mitochondrial transmembrane potential, permeabilizes the plasma membrane, and decreases the viability of hepatoma tissue culture cells *in vitro* (57). Amitriptyline is a tricyclic antidepressant drug that inhibits the activities of mitochondrial complex III and stimulates the generation of reactive oxygen species in human hepatoma cells (59). Other identified drugs, including nordihydroguaiaretic acid, alexidine, and celastrol, induce mitochondrial apoptosis in cancer cells (35, 39, 60).

Although we did not investigate the cytotoxic effects of the identified drugs, one of the limitations of using these inhibitors as antimicrobials is that they may target mitochondria in humans. Nordihydroguaiaretic acid treatment inhibited the oxidative stress-induced damage of primary neuron cells by improving their ATP generation and mitochondrial morphology and function in a dose-dependent manner ($<$10 μM) (61). However, it did not offer a protective effect on the neuron cells at a concentration higher than 10 μM (61). Cell survival assays revealed a robust cytotoxic potency of nordihydroguaiaretic acid and its analogs against four cell lines (62). An *in vivo* study revealed that gossypol's lethal dose (2400 mg/kg body weight) is exceptionally high in a rat model, suggesting its lower toxicity against normal tissue (63). Trifluoperazine, an antipsychotic drug, is orally administrable, which blocks the dopamine receptors (64). Ganapathi et al. showed that, at a noncytotoxic concentration (5 μM), trifluoperazine sensitized doxorubicin-resistant mouse melanoma cells to doxorubicin (65). However, in the case of prolonged treatments, trifluoperazine can become cytotoxic against normal cells (66). Extensive research is required to further elucidate these drugs' effects against mammalian cells and their mitochondria, although previous studies suggest that a considerably higher dose is required to damage the mammalian cells. Even traditional antibiotics at higher doses inhibit mammalian cell growth and metabolic activity and impair mitochondrial functions (67).

Our screening assay identified a number of drugs that were highly effective against MRSA cells. In *Escherichia coli*, trifluoperazine irreversibly inhibits ATP synthase by interacting with the F0 and F1 subunits (68). Amitriptyline inhibits the AcrB multidrug efflux pump in *Salmonella* Typhimurium and *E. coli* strains (69) and kills drug-resistant Gram-positive and -negative bacteria when used as an antibiotic adjuvant (70). Nordihydroguaiaretic acid disrupts the cytoplasmic membrane and reduces intracellular ATP levels of *S. aureus* (71). Alexidine has broad-spectrum activities against *Enterococcus faecalis* biofilm infections and fungal pathogens (72). However, the exact molecular mechanism of action of alexidine against bacteria has yet to be elucidated. Diclofenac inhibits DNA synthesis in *E. coli* and *S. aureus* and exhibits antibacterial activity (73). In addition, celastrol treatment makes *B. subtilis* cells elongated and spindle-shaped. Using transmission electron microscopy, celastrol has been shown to damage cell membranes to a certain extent (74).

Most PMF inhibitors have complex modes of action, making cross-species comparisons difficult. In *E. coli*, thioridazine was previously shown to selectively dissipate ΔpH by potentially interacting with membrane-bound proteins associated with energy metabolism, such as succinate:quinone oxidoreductase (SdhA, SdhB, SdhC, and SdhD); cytochrome bd-I ubiquinol

oxidase (CydX); and NADH:quinone oxidoreductase complexes (NuoJ and NuoF) (75). However, our current study demonstrated that thioridazine disrupts $\Delta\Psi$ in Gram-positive bacteria, underlining the existence of distinct mechanisms across species. Culture conditions (e.g., inhibitor concentrations and the timing of inhibitor addition), redundant interactions between the inhibitors and cellular components, the existence or absence of an outer membrane, and the thickness of peptidoglycans may affect the cellular responses to treatments. Moreover, we found that lower concentrations (5× MIC) of thioridazine, CCCP, FCCP, trifluoperazine, amitriptyline, diclofenac, and celastrol disrupted cellular PMF more than higher concentrations (10× MIC). These PMF inhibitors disrupt $\Delta\Psi$, and we did not observe the same phenomenon for inhibitors that selectively dissipate ΔpH, which warrants further investigation.

In conclusion, we demonstrate that PMF inhibitors can be highly effective bactericidal antibiotics with the potential to eradicate antibiotic-tolerant cells. Our statistical analysis verified that inhibitors that enhance PMF disruption and cell membrane permeabilization could be potent bactericidal drugs. The outcomes of this study also support the use of screening strategies (9) for the development of novel drugs that selectively target bacterial PMF.

MATERIALS AND METHODS

Bacterial strains, chemicals, and culture conditions. The strains MRSA BAA-41 and MRSA 700699 used in this study were obtained from Kevin W. Garey at the University of Houston (47, 48). The chemicals were purchased from Fisher Scientific (Atlanta, GA), VWR International (Pittsburg, PA), or Sigma-Aldrich (St. Louis, MO). The MitoPlate I-1 (catalog no. 14104) used for chemical screening (Table S3) was obtained from Biolog, Inc. (Hayward, CA). The chemical library contained four different concentrations (C_1, C_2, C_3, and C_4) for each drug. However, these concentrations were not disclosed by the vendor. Mueller-Hinton broth (2.0 g beef extract powder, 17.5 g acid digest of casein, and 1.5 g soluble starch in 1 liter deionized [DI] water) was used to grow the MRSA strains. To enumerate the CFU, Mueller-Hinton agar (2.0 g beef extract powder, 17.5 g acid digest of casein, 1.5 g soluble starch, and 17.0 g agar in 1 liter DI water) was used. Treated cells were washed with 1× phosphate-buffered saline (PBS) solution to lower the concentrations of antibiotics and chemicals below their MICs. Conventional antibiotics (kanamycin, ampicillin, ofloxacin, ciprofloxacin, fosfomycin, and vancomycin), known PMF inhibitors (CCCP, polymyxin B, and thioridazine), and the hit chemicals obtained from the screening assay (alexidine, nordihydroguaiaretic acid, FCCP, diclofenac, celastrol, gossypol, trifluoperazine, and amitriptyline) were used at 5× and 10× MIC to treat the MRSA strains. These two concentrations were chosen since drug treatment at MIC is not clinically relevant (76). In addition, antibiotic-tolerant or -resistant cells have the ability to survive high concentrations of antibiotics (49, 77, 78). MICs of antibiotics and identified chemicals for the two strains are provided in Table 1 and Table S1 (A, B). The Etest strip method was used to determine the MICs of kanamycin, ampicillin, ofloxacin, ciprofloxacin, fosfomycin, and vancomycin. A 2-fold serial dilution (macrodilution) method was used to detect the MICs of CCCP, polymyxin B, thioridazine, alexidine, nordihydroguaiaretic acid, FCCP, diclofenac, celastrol, gossypol, trifluoperazine, and amitriptyline (46). The vendor, catalog, and purity information of all chemicals is listed in Table S4. The solvents and stock solution concentrations of chemicals are tabulated in Table S5. Chemicals dissolved in DI water were sterilized with 0.2-μm syringe filters. An autoclave was used to sterilize the liquid and solid media. Overnight precultures were prepared by inoculating cells from a 25% glycerol cell stock (stored at −80°C) in a 14-mL round-bottom Falcon test tube containing 2 mL Mueller-Hinton broth and cultured at 37°C for 24 h in an orbital shaker at 250 rpm (rpm). Main cultures were prepared by diluting overnight precultures 100-fold into 2 mL fresh Mueller-Hinton medium in 14-mL test tubes. Unless otherwise stated, chemical treatments were performed at the exponential phase (OD_{600} of ~0.1) for 6 h. The shaker speed and temperature were kept constant (250 rpm and 37°C) in all experiments.

Cell growth and clonogenic survival assays. Overnight precultures were diluted 100-fold in 14-mL test tubes containing 2 mL Mueller-Hinton medium and grown in the shaker. At indicated time points, cell samples were collected to measure OD_{600} with a Varioskan LUX Multimode Microplate Reader (Thermo Fisher, Waltham, MA, USA). When the cultures reached an OD_{600} of 0.1, the cells were treated with antibiotics or chemicals at 5× and 10× MIC. At designated time points, 200-μL treated cultures were collected and diluted in 800 μL sterile PBS. Diluted cell cultures were then washed twice with PBS by centrifugation at 13,300 rpm (17,000 × *g*) for 3 min to remove the antibiotics and chemicals, as described elsewhere (79). After the final centrifugation, 900 μL supernatant was removed, and the pelleted cells were resuspended in the remaining 100 μL, which was then used for a 10-fold serial dilution in 90 μL PBS. 10 μL of diluted cells were then spotted on Mueller-Hinton agar. Ninety μL of undiluted cell suspension were also plated on Mueller-Hinton agar to increase the limit of detection (which is equivalent to ~5 CFU/mL). After incubation of the agar plates for 16 h at 37°C, CFU were counted to determine the cell survival levels. Incubations longer than 16 h did not increase the CFU levels.

$DiSC_3(5)$ assay. Overnight precultures were diluted 100-fold in 14-mL test tubes containing 2 mL fresh Mueller-Hinton broth and grown at 37°C with shaking (250 rpm). Exponential-phase cells (OD_{600} of ~0.1) were collected, washed three times with a buffer solution (50 mM HEPES, 300 mM KCl, and 0.1% glucose), and centrifuged at 13,300 rpm (13). After the final washing step, pelleted cells were resuspended in 2 mL buffer, loaded with 1 μM $DiSC_3(5)$ dye, and incubated in the dark. The fluorescence levels were measured with a plate reader at 620-nm excitation and 670-nm emission wavelengths every 10 min. When the fluorescence levels

reached an equilibrium state (after 30 min), stained cells were treated with chemicals at indicated concentrations and incubated in the dark. At designated time points, 200 μL cells were collected to measure the fluorescence levels. Cultures that did not receive any chemical treatment served as controls.

Chemical screening assay. Overnight precultures were diluted 100-fold in 14-mL test tubes containing 2 mL fresh Mueller-Hinton broth and grown at 37°C with shaking (250 rpm). Cells at an OD_{600} of ~0.1 were collected and washed three times in buffer (50 mM HEPES, 300 mM KCl, and 0.1% glucose) with centrifugation at 13,300 rpm. After the final washing step, pelleted cells were resuspended in buffer, loaded with 1 μM $DiSC_3(5)$ dye, and incubated in the dark. Once the fluorescence levels reached a steady-state (after 30 min), 100 μL stained cells were transferred to each well of the MitoPlate I-1 preloaded with chemicals (Table S3) and incubated in the dark. The fluorescence level of each well was measured with the plate reader at designated time points. Wells without chemicals (A1 to A8) served as controls.

PI staining. Overnight precultures were diluted 100-fold in 14-mL test tubes containing 2 mL fresh Mueller-Hinton broth and grown at 37°C with shaking. Cells at an OD_{600} of ~0.1 were treated with the chemicals at indicated concentrations for 1 h. Treated cells were then collected and diluted in 0.85% NaCl solution in flow cytometry tubes (5-mL round-bottom Falcon tubes) to obtain a final cell density of ~10^6 cells/mL. The resulting cell suspensions were stained with 20 μM PI dye and incubated at 37°C in the dark for 15 min. Stained cells were collected and analyzed with a flow cytometer (NovoCyte Flow Cytometer, NovoCyte 3000RYB, ACEA Biosciences Inc., San Diego, CA, USA). Ethanol (70% vol/vol)-treated cells (i.e., dead cells) were used as a positive control (PI-positive cells), and PI-stained live cells (PI-negative cells) served as a negative control (Fig. S2). Forward and side scatter parameters obtained from the untreated live cells were used to gate the cell populations on the flow cytometry diagram (80). For the fluorescence measurement, the cells were excited at a 561-nm wavelength and detected with a 615/20-nm bandpass filter.

Multivariable linear regression analysis. Multivariable linear regression analysis was performed to determine correlations between the response (cell survival levels) and independent variables (PMF disruption and membrane permeability). The CFU/mL, PMF, and membrane permeabilization data sets used here correspond to the last time points of the related assays. Log-transformed values of CFU/mL obtained from clonogenic survival assays were defined as cell survival levels. PMF disruption was defined as the fold change in $DiSC_3(5)$ fluorescence levels between treated and untreated cells, and membrane permeability was defined as the percentage of PI-positive cells in the flow cytometry diagram. GraphPad Prism 9.3.0 was used to perform the multiple linear regression analysis. The linear model equations without and with a two-way interaction are as follows, respectively:

$$P_L = \beta_0 + \beta_1 \times P_D + \beta_2 \times P_M$$

$$P_L = \beta_0 + \beta_1 \times P_D + \beta_2 \times P_M + \beta_3 \times P_D \times P_M$$

In these equations, P_L is the log-transformed value of the cell survival levels, P_D is PMF disruption, P_M is membrane permeability, β_0 is the estimate of the model intercept, β_1 is the estimate of the model coefficient of PMF disruption, β_2 is the estimate of the model coefficient of membrane permeability, and β_3 is the estimate of the model coefficient of the interaction term. The parameters identified from the regression analysis were used to generate three-dimensional plots with MATLAB. Quantile-quantile (QQ) probability plots were generated to check the normality of the data set (Fig. S10A, B).

Data analysis. Unless stated otherwise, at least three independent biological replicates were performed for each experiment. FlowJo (version 10.8.1) software was used to analyze the flow cytometry data. Each data point in the figures denotes the mean value, and error bars represent the standard deviation (SD). F statistics were used to determine significant differences between the model equations. Student's *t* tests with unequal variance were performed to determine the statistical significance between two groups. The *P* value thresholds were selected as follows: *, $P < 0.01$; **, $P < 0.001$; ***, $P < 0.0001$, and ns, not significant.

SUPPLEMENTAL MATERIAL

Supplemental material is available online only.

SUPPLEMENTAL FILE 1, PDF file, 3.7 MB.

ACKNOWLEDGMENTS

We thank the Orman Lab members for their help.

This study was supported by NIAID, National Institutes of Health award R01 AI143643 and a University of Houston startup grant.

S.G.M., S.G., P.K., and M.A.O. conceived and designed the study. S.G.M., S.G., and P.K. performed the experiments. S.G.M., S.G., and M.A.O. analyzed the data and wrote the paper. All authors have read and approved the manuscript.

We declare no conflict of interests.

Data supporting the conclusions of this article will be made available by the authors to any qualified researcher upon request.

REFERENCES

1. Otto M. 2013. Community-associated MRSA: what makes them special? Int J Med Microbiol 303:324–330. https://doi.org/10.1016/j.ijmm.2013.02.007.
2. Strauß L, Stegger M, Akpaka PE, Alabi A, Breurec S, Coombs G, Egyir B, Larsen AR, Laurent F, Monecke S, Peters G, Skov R, Strommenger B, Vandenesch F, Schaumburg F, Mellmann A. 2017. Origin, evolution, and global transmission of community-acquired *Staphylococcus aureus* ST8. Proc Natl Acad Sci U S A 114:E10596–E10604. https://doi.org/10.1073/pnas.1702472114.
3. Jevons MP. 1961. Celbenin-resistant staphylococci. Br Med J 1:124–125. https://doi.org/10.1136/bmj.1.5219.124-a.
4. Hiramatsu K, Cui L, Kuroda M, Ito T. 2001. The emergence and evolution of methicillin-resistant *Staphylococcus aureus*. Trends Microbiol 9:486–493. https://doi.org/10.1016/s0966-842x(01)02175-8.
5. Rello J, Sole-Violan J, Sa-Borges M, Garnacho-Montero J, Muñoz E, Sirgo G, Olona M, Diaz E. 2005. Pneumonia caused by oxacillin-resistant *Staphylococcus aureus* treated with glycopeptides. Crit Care Med 33:1983–1987. https://doi.org/10.1097/01.CCM.0000178180.61305.1D.
6. Klevens RM, Morrison MA, Nadle J, Petit S, Gershman K, Ray S, Harrison LH, Lynfield R, Dumyati G, Townes JM, Craig AS, Zell ER, Fosheim GE, McDougal LK, Carey RB, Fridkin SK, Active Bacterial Core Surveillance (ABCs) MRSA Investigators. 2007. Invasive methicillin-resistant *Staphylococcus aureus* infections in the United States. JAMA 298:1763–1771. https://doi.org/10.1001/jama.298.15.1763.
7. Horan TC, Culver DH, Gaynes RP, Jarvis WR, Edwards JR, Reid CR, National Nosocomial Infections Surveillance (NNIS) System. 1993. Nosocomial infections in surgical patients in the United States, January 1986–June 1992. Infect Control Hosp Epidemiol 14:73–80. https://doi.org/10.2307/30147164.
8. Brady RA, O'May GA, Leid JG, Prior ML, Costerton JW, Shirtliff ME. 2011. Resolution of *Staphylococcus aureus* biofilm infection using vaccination and antibiotic treatment. Infect Immun 79:1797–1803. https://doi.org/10.1128/IAI.00451-10.
9. Farha MA, Verschoor CP, Bowdish D, Brown ED. 2013. Collapsing the proton motive force to identify synergistic combinations against *Staphylococcus aureus*. Chem Biol 20:1168–1178. https://doi.org/10.1016/j.chembiol.2013.07.006.
10. Mates SM, Patel L, Kaback HR, Miller MH. 1983. Membrane potential in anaerobically growing *Staphylococcus aureus* and its relationship to gentamicin uptake. Antimicrob Agents Chemother 23:526–530. https://doi.org/10.1128/AAC.23.4.526.
11. Bakker EP, Mangerich WE. 1981. Interconversion of components of the bacterial proton motive force by electrogenic potassium transport. J Bacteriol 147:820–826. https://doi.org/10.1128/jb.147.3.820-826.1981.
12. Kim W, Hendricks GL, Tori K, Fuchs BB, Mylonakis E. 2018. Strategies against methicillin-resistant *Staphylococcus aureus* persisters. Future Med Chem 10:779–794. https://doi.org/10.4155/fmc-2017-0199.
13. Stokes JM, Yang K, Swanson K, Jin W, Cubillos-Ruiz A, Donghia NM, MacNair CR, French S, Carfrae LA, Bloom-Ackerman Z, Tran VM, Chiappino-Pepe A, Badran AH, Andrews IW, Chory EJ, Church GM, Brown ED, Jaakkola TS, Barzilay R, Collins JJ. 2020. A deep learning approach to antibiotic discovery. Cell 180:688–702.e13. https://doi.org/10.1016/j.cell.2020.01.021.
14. Dombach JL, Quintana JLJ, Detweiler CS. 2021. Staphylococcal bacterial persister cells, biofilms, and intracellular infection are disrupted by JD1, a membrane-damaging small molecule. mBio 12:e01801-21. https://doi.org/10.1128/mBio.01801-21.
15. Hasenoehrl EJ, Wiggins TJ, Berney M. 2021. Bioenergetic inhibitors: antibiotic efficacy and mechanisms of action in *Mycobacterium tuberculosis*. Front Cell Infect Microbiol 10:815. https://www.frontiersin.org/articles/10.3389/fcimb.2020.611683/full.
16. Feng X, Zhu W, Schurig-Briccio LA, Lindert S, Shoen C, Hitchings R, Li J, Wang Y, Baig N, Zhou T, Kim BK, Crick DC, Cynamon M, McCammon JA, Gennis RB, Oldfield E. 2015. Antiinfectives targeting enzymes and the proton motive force. Proc Natl Acad Sci U S A 112:E7073–E7082. https://www.pnas.org/doi/10.1073/pnas.1521988112.
17. Foss MH, Eun YJ, Grove CI, Pauw DA, Sorto NA, Rensvold JW, Pagliarini DJ, Shaw JT, Weibel DB. 2013. Inhibitors of bacterial tubulin target bacterial membranes *in vivo*. Medchemcomm 4:112–119. https://doi.org/10.1039/C2MD20127E.
18. Weinstein EA, Yano T, Li LS, Avarbock D, Avarbock A, Helm D, McColm AA, Duncan K, Lonsdale JT, Rubin H. 2005. Inhibitors of type II NADH:menaquinone oxidoreductase represent a class of antitubercular drugs. Proc Natl Acad Sci U S A 102:4548–4553. https://doi.org/10.1073/pnas.0500469102.
19. French S, Farha M, Ellis MJ, Sameer Z, Côté JP, Cotroneo N, Lister T, Rubio A, Brown ED. 2020. Potentiation of antibiotics against Gram-negative bacteria by polymyxin B analogue SPR741 from unique perturbation of the outer membrane. ACS Infect Dis 6:1405–1412. https://doi.org/10.1021/acsinfecdis.9b00159.
20. Nonejuie P, Burkart M, Pogliano K, Pogliano J. 2013. Bacterial cytological profiling rapidly identifies the cellular pathways targeted by antibacterial molecules. Proc Natl Acad Sci U S A 110:16169–16174. https://doi.org/10.1073/pnas.1311066110.
21. Bruno MEC, Kaiser A, Montville TJ. 1992. Depletion of proton motive force by nisin in *Listeria monocytogenes* cells. Appl Environ Microbiol 58:2255–2259. https://doi.org/10.1128/aem.58.7.2255-2259.1992.
22. Borselli D, Brunel JM, Gorgé O, Bolla JM. 2019. Polyamino-isoprenyl derivatives as antibiotic adjuvants and motility inhibitors for *Bordetella bronchiseptica* porcine pulmonary infection treatment. Front Microbiol 10:1771. https://doi.org/10.3389/fmicb.2019.01771.
23. Machado D, Fernandes L, Costa SS, Cannalire R, Manfroni G, Tabarrini O, Couto I, Sabatini S, Viveiros M. 2017. Mode of action of the 2-phenylquinoline efflux inhibitor PQQ4R against *Escherichia coli*. PeerJ 5:e3168. https://doi.org/10.7717/peerj.3168.
24. Trimble MJ, Mlynárčik P, Kolář M, Hancock REW. 2016. Polymyxin: alternative mechanisms of action and resistance. Cold Spring Harb Perspect Med 6:a025288. https://doi.org/10.1101/cshperspect.a025288.
25. Boshoff HIM, Myers TG, Copp BR, McNeil MR, Wilson MA, Barry CE. 2004. The transcriptional responses of *Mycobacterium tuberculosis* to inhibitors of metabolism: novel insights into drug mechanisms of action. J Biol Chem 279:40174–40184. https://doi.org/10.1074/jbc.M406796200.
26. Strahl H, Hamoen LW. 2010. Membrane potential is important for bacterial cell division. Proc Natl Acad Sci U S A 107:12281–12286. https://doi.org/10.1073/pnas.1005485107.
27. Jovanovic G, Lloyd LJ, Stumpf MPH, Mayhew AJ, Buck M. 2006. Induction and function of the phage shock protein extracytoplasmic stress response in *Escherichia coli*. J Biol Chem 281:21147–21161. https://doi.org/10.1074/jbc.M602323200.
28. Krause KM, Serio AW, Kane TR, Connolly LE. 2016. Aminoglycosides: an overview. Cold Spring Harb Perspect Med 6:a027029. https://doi.org/10.1101/cshperspect.a027029.
29. Iovine NM. 2013. Resistance mechanisms in *Campylobacter jejuni*. Virulence 4:230–240. https://doi.org/10.4161/viru.23753.
30. Lewin CS, Smith JT. 1988. Bactrecidal mechanisms of ofloxacin. J Antimicrob Chemother 22:1–8. https://doi.org/10.1093/jac/22.Supplement_C.1.
31. Silver LL. 2017. Fosfomycin: mechanism and resistance. Cold Spring Harb Perspect Med 7:a025262. https://doi.org/10.1101/cshperspect.a025262.
32. Watanakunakorn C. 1984. Mode of action and *in-vitro* activity of vancomycin. J Antimicrob Chemother 14:7–18. https://doi.org/10.1093/jac/14.suppl_D.7.
33. Li N, Ragheb K, Lawler G, Sturgis J, Rajwa B, Melendez JA, Robinson JP. 2003. Mitochondrial complex I inhibitor rotenone induces apoptosis through enhancing mitochondrial reactive oxygen species production. J Biol Chem 278:8516–8525. https://doi.org/10.1074/jbc.M210432200.
34. Valls-Lacalle L, Barba I, Miró-Casas E, Alburquerque-Béjar JJ, Ruiz-Meana M, Fuertes-Agudo M, Rodríguez-Sinovas A, García-Dorado D. 2016. Succinate dehydrogenase inhibition with malonate during reperfusion reduces infarct size by preventing mitochondrial permeability transition. Cardiovasc Res 109:374–384. https://doi.org/10.1093/cvr/cvv279.
35. Chen G, Zhang X, Zhao M, Wang Y, Cheng X, Wang D, Xu Y, Du Z, Yu X. 2011. Celastrol targets mitochondrial respiratory chain complex I to induce reactive oxygen species-dependent cytotoxicity in tumor cells. BMC Cancer 11:170–113. https://doi.org/10.1186/1471-2407-11-170.
36. Arinbasarova AY, Medentsev AG, Krupyanko VI. 2012. Gossypol inhibits electron transport and stimulates ROS generation in *Yarrowia lipolytica* mitochondria. Open Biochem J 6:11–15. https://doi.org/10.2174/1874091X01206010011.
37. Ma X, Jin M, Cai Y, Xia H, Long K, Liu J, Yu Q, Yuan J. 2011. Mitochondrial electron transport chain complex III is required for antimycin A to inhibit autophagy. Chem Biol 18:1474–1481. https://doi.org/10.1016/j.chembiol.2011.08.009.
38. Navarro A, Bández MJ, Gómez C, Repetto MG, Boveris A. 2010. Effects of rotenone and pyridaben on complex I electron transfer and on mitochondrial nitric oxide synthase functional activity. J Bioenerg Biomembr 42:405–412. https://doi.org/10.1007/s10863-010-9309-4.
39. Doughty-Shenton D, Joseph JD, Zhang J, Pagliarini DJ, Kim Y, Lu D, Dixon JE, Casey PJ. 2010. Pharmacological targeting of the mitochondrial phosphatase PTPMT1. J Pharmacol Exp Ther 333:584–592. https://doi.org/10.1124/jpet.109.163329.
40. Weinberg SE, Chandel NS. 2015. Targeting mitochondria metabolism for cancer therapy. Nat Chem Biol 11:9–15. https://doi.org/10.1038/nchembio.1712.
41. Desquiret V, Loiseau D, Jacques C, Douay O, Malthièry Y, Ritz P, Roussel D. 2006. Dinitrophenol-induced mitochondrial uncoupling *in vivo* triggers respiratory adaptation in HepG2 cells. Biochim Biophys Acta 1757:21–30. https://doi.org/10.1016/j.bbabio.2005.11.005.

42. Syed M, Skonberg C, Hansen SH. 2016. Mitochondrial toxicity of diclofenac and its metabolites via inhibition of oxidative phosphorylation (ATP synthesis) in rat liver mitochondria: possible role in drug induced liver injury (DILI). Toxicol in Vitro 31:93–102. https://doi.org/10.1016/j.tiv.2015.11.020.
43. Hamman WM, Spencer M. 1977. Relationship of potassium ion transport and ATP synthesis in pea cotyledon mitochondria. Can J Biochem 55:376–383. https://doi.org/10.1139/o77-052.
44. Lemasters JJ, Theruvath TP, Zhong Z, Nieminen AL. 2009. Mitochondrial calcium and the permeability transition in cell death. Biochim Biophys Acta 1787:1395–1401. https://doi.org/10.1016/j.bbabio.2009.06.009.
45. Kracke F, Vassilev I, Krömer JO. 2015. Microbial electron transport and energy conservation—the foundation for optimizing bioelectrochemical systems. Front Microbiol 6:575. https://doi.org/10.3389/fmicb.2015.00575.
46. Andrews JM. 2001. Determination of minimum inhibitory concentrations. J Antimicrob Chemother 48:5–16. https://doi.org/10.1093/jac/48.suppl_1.5.
47. Monecke S, Coombs G, Shore AC, Coleman DC, Akpaka P, Borg M, Chow H, Ip M, Jatzwauk L, Jonas D, Kadlec K, Kearns A, Laurent F, O'Brien FG, Pearson J, Ruppelt A, Schwarz S, Scicluna E, Slickers P, Tan H-L, Weber S, Ehricht R. 2011. A field guide to pandemic, epidemic and sporadic clones of methicillin-resistant *Staphylococcus aureus*. PLoS One 6:e17936. https://doi.org/10.1371/journal.pone.0017936.
48. Hiramatsu K, Aritaka N, Hanaki H, Kawasaki S, Hosoda Y, Hori S, Fukuchi Y, Kobayashi I. 1997. Dissemination in Japanese hospitals of strains of *Staphylococcus aureus* heterogeneously resistant to vancomycin. Lancet 350:1670–1673. https://doi.org/10.1016/S0140-6736(97)07324-8.
49. Levin-Reisman I, Brauner A, Ronin I, Balaban NQ. 2019. Epistasis between antibiotic tolerance, persistence, and resistance mutations. Proc Natl Acad Sci U S A 116:14734–14739. https://doi.org/10.1073/pnas.1906169116.
50. Brauner A, Fridman O, Gefen O, Balaban NQ. 2016. Distinguishing between resistance, tolerance and persistence to antibiotic treatment. Nat Rev Microbiol 14:320–330. https://doi.org/10.1038/nrmicro.2016.34.
51. Handwerger S, Tomasz A. 1985. Antibiotic tolerance among clinical isolates of bacteria. Rev Infect Dis 7:368–386. https://doi.org/10.1093/clinids/7.3.368.
52. Depardieu F, Podglajen I, Leclercq R, Collatz E, Courvalin P. 2007. Modes and modulations of antibiotic resistance gene expression. Clin Microbiol Rev 20:79–114. https://doi.org/10.1128/CMR.00015-06.
53. Blair JMA, Webber MA, Baylay AJ, Ogbolu DO, Piddock LJV. 2015. Molecular mechanisms of antibiotic resistance. Nat Rev Microbiol 13:42–51. https://doi.org/10.1038/nrmicro3380.
54. Balaban NQ, Helaine S, Lewis K, Ackermann M, Aldridge B, Andersson DI, Brynildsen MP, Bumann D, Camilli A, Collins JJ, Dehio C, Fortune S, Ghigo JM, Hardt WD, Harms A, Heinemann M, Hung DT, Jenal U, Levin BR, Michiels J, Storz G, Tan MW, Tenson T, Van Melderen L, Zinkernagel A. 2019. Definitions and guidelines for research on antibiotic persistence. Nat Rev Microbiol 17:441–448. https://doi.org/10.1038/s41579-019-0196-3.
55. Gohil VM, Zhu L, Baker CD, Cracan V, Yaseen A, Jain M, Clish CB, Brookes PS, Bakovic M, Mootha VK. 2013. Meclizine inhibits mitochondrial respiration through direct targeting of cytosolic phosphoethanolamine metabolism. J Biol Chem 288:35489–35499. https://www.sciencedirect.com/science/article/pii/S0021925820554033.
56. Pereira CV, Machado NG, Oliveira PJ. 2008. Mechanisms of berberine (natural yellow 18)–induced mitochondrial dysfunction: interaction with the adenine nucleotide translocator. Toxicol Sci 105:408–417. https://doi.org/10.1093/toxsci/kfn131.
57. de Faria PA, Bettanin F, Cunha RLOR, Paredes-Gamero EJ, Homem-de-Mello P, Nantes IL, Rodrigues T. 2015. Cytotoxicity of phenothiazine derivatives associated with mitochondrial dysfunction: a structure-activity investigation. Toxicology 330:44–54. https://doi.org/10.1016/j.tox.2015.02.004.
58. Lin J, Wu Y, Yang D, Zhao Y. 2013. Induction of apoptosis and antitumor effects of a small molecule inhibitor of Bcl-2 and Bcl-xl, gossypol acetate, in multiple myeloma *in vitro* and *in vivo*. Oncol Rep 30:731–738. https://doi.org/10.3892/or.2013.2489.
59. Villanueva-Paz M, Cordero MD, Pavón AD, Vega BC, Cotán D, De la Mata M, Oropesa-Ávila M, Alcocer-Gomez E, de Lavera I, Garrido-Maraver J, Carrascosa J, Zaderenko AP, Muntané J, de Miguel M, Sánchez-Alcázar JA. 2016. Amitriptyline induces mitophagy that precedes apoptosis in human HepG2 cells. Genes Cancer 7:260–277. https://doi.org/10.18632/genesandcancer.114.
60. Biswal SS, Datta K, Shaw SD, Feng X, Robertson JD, Kehrer JP. 2000. Glutathione oxidation and mitochondrial depolarization as mechanisms of nordihydroguaiaretic acid-induced apoptosis in lipoxygenase-deficient FL5.12 cells. Toxicol Sci 53:77–83. https://doi.org/10.1093/toxsci/53.1.77.
61. Lee J, Kosaras B, Del Signore SJ, Cormier K, McKee A, Ratan RR, Kowall NW, Ryu H. 2011. Modulation of lipid peroxidation and mitochondrial function by nordihydroguaiaretic acid (NDGA) improves neuropathology in Huntington's disease mice. Acta Neuropathol 121:487–498. https://doi.org/10.1007/s00401-010-0788-5.
62. Meyers RO, Lambert JD, Hajicek N, Pourpak A, Kalaitzis JA, Dorr RT. 2009. Synthesis, characterization and anti-melanoma activity of tetra-*O*-substituted analogs of nordihydroguaiaretic acid. Bioorg Med Chem Lett 19:4752–4755. https://doi.org/10.1016/j.bmcl.2009.06.063.
63. El-Nockrashy AS, Lyman CM, Dollahite JW. 1963. The acute oral toxicity of cottonseed pigment glands and intraglandular pigments. J Am Oil Chem Soc 40:14–17. https://doi.org/10.1007/BF02645780.
64. Ohlow MJ, Moosmann B. 2011. Phenothiazine: the seven lives of pharmacology's first lead structure. Drug Discov Today 16:119–131. https://doi.org/10.1016/j.drudis.2011.01.001.
65. Ganapathi R, Grabowski D, Rouse W, Riegler F. 1984. Differential effect of the calmodulin inhibitor trifluoperazine on cellular accumulation, retention, and cytotoxicity of anthracyclines in doxorubicin (adriamycin)-resistant P388 mouse leukemia cells. Cancer Res 44:5056–5061. https://www.sciencedirect.com/science/article/abs/pii/0006295288907162.
66. Borsa J, Einspenner M, Sargent MD, Hickie RA. 1986. Selective cytotoxicity of calmidazolium and trifluoperazine for cycling versus noncycling C3H10T1/2 cells *in vitro*. Cancer Res 46:133–136.
67. Duewelhenke N, Krut O, Eysel P. 2007. Influence on mitochondria and cytotoxicity of different antibiotics administered in high concentrations on primary human osteoblasts and cell lines. Antimicrob Agents Chemother 51:54–63. https://doi.org/10.1128/AAC.00729-05.
68. Dabbeni-Sala F, Schiavo G, Palatini P. 1990. Mechanism of local anesthetic effect on mitochondrial ATP synthase as deduced from photolabelling and inhibition studies with phenothiazine derivatives. Biochim Biophys Acta Biomembr 1026:117–125. https://doi.org/10.1016/0005-2736(90)90341-K.
69. Grimsey EM, Fais C, Marshall RL, Ricci V, Ciusa ML, Stone JW, Ivens A, Malloci G, Ruggerone P, Vargiu AV, Piddock LJV. 2020. Chlorpromazine and amitriptyline are substrates and inhibitors of the acrb multidrug efflux pump. mBio 11:e00465-20. https://doi.org/10.1128/mBio.00465-20.
70. Mohiuddin SG, Hoang T, Saba A, Karki P, Orman MA. 2020. Identifying metabolic inhibitors to reduce bacterial persistence. Front Microbiol 11:472. https://doi.org/10.3389/fmicb.2020.00472.
71. Cunningham-Oakes E, Soren O, Moussa C, Rathor G, Liu Y, Coates A, Hu Y. 2015. Nordihydroguaiaretic acid enhances the activities of aminoglycosides against methicillin-sensitive and resistant *Staphylococcus aureus in vitro* and *in vivo*. Front Microbiol 6:1195. https://doi.org/10.3389/fmicb.2015.01195.
72. Mamouei Z, Alqarihi A, Singh S, Xu S, Mansour MK, Ibrahim AS, Uppuluri P. 2018. Alexidine dihydrochloride has broad-spectrum activities against diverse fungal pathogens. mSphere 3:e00539-18. https://doi.org/10.1128/mSphere.00539-18.
73. Dastidar SG, Ganguly K, Chaudhuri K, Chakrabarty AN. 2000. The anti-bacterial action of diclofenac shown by inhibition of DNA synthesis. Int J Antimicrob Agents 14:249–251. https://doi.org/10.1016/S0924-8579(99)00159-4.
74. Padilla-Montaño N, Guerra L de L, Moujir L. 2021. Antimicrobial activity and mode of action of celastrol, a nortriterpen quinone isolated from natural sources. Foods 10:591. https://doi.org/10.3390/foods10030591.
75. Mohiuddin SG, Nguyen TV, Orman MA. 2022. Pleiotropic actions of phenothiazine drugs are detrimental to Gram-negative bacterial persister cells. Commun Biol 5:1–15. https://doi.org/10.1038/s42003-022-03172-8.
76. Kowalska-Krochmal B, Dudek-Wicher R. 2021. The minimum inhibitory concentration of antibiotics: methods, interpretation, clinical relevance. Pathog 10:165. https://doi.org/10.3390/pathogens10020165.
77. Levin-Reisman I, Ronin I, Gefen O, Braniss I, Shoresh N, Balaban NQ. 2017. Antibiotic tolerance facilitates the evolution of resistance. Science 355:826–830. https://doi.org/10.1126/science.aaj2191.
78. Wang M, Chan EWC, Wan Y, Wong MH, Chen S. 2021. Active maintenance of proton motive force mediates starvation-induced bacterial antibiotic tolerance in *Escherichia coli*. Commun Biol 4:1–11. https://doi.org/10.1038/s42003-021-02612-1.
79. Mohiuddin SG, Kavousi P, Orman MA. 2020. Flow-cytometry analysis reveals persister resuscitation characteristics. BMC Microbiol 20:202–213. https://doi.org/10.1186/s12866-020-01888-3.
80. Mohiuddin SG, Orman MA. 2021. Monitoring persister resuscitation with flow cytometry. Methods Mol Biol 2357:209–222. https://doi.org/10.1007/978-1-0716-1621-5_14.